

# 行政院國家科學委員會專題研究計畫 成果報告

## 片狀矽酸鹽/高分子熔融懸浮液之光學流變研究

計畫類別：個別型計畫

計畫編號：NSC94-2216-E-029-001-

執行期間：94年08月01日至95年07月31日

執行單位：東海大學化學工程學系

計畫主持人：楊怡寬

計畫參與人員：朱炯龍，劉佳芸，蔡秉宏

報告類型：精簡報告

報告附件：出席國際會議研究心得報告及發表論文

處理方式：本計畫可公開查詢

中 華 民 國 95 年 10 月 30 日

行政院國家科學委員會補助專題研究計畫  成果報告  
 期中進度報告

片狀矽酸鹽/高分子熔融懸浮之光學流變研究

計畫類別： 個別型計畫  整合型計畫

計畫編號：NSC 94-2216-E-029-001-

執行期間：94年8月1日至95年7月31日

計畫主持人：楊怡寬教授

共同主持人：

計畫參與人員：朱炯龍、劉佳芸、蔡秉宏

成果報告類型(依經費核定清單規定繳交)： 精簡報告  完整報告

本成果報告包括以下應繳交之附件：

赴國外出差或研習心得報告一份

赴大陸地區出差或研習心得報告一份

出席國際學術會議心得報告及發表之論文各一份

國際合作研究計畫國外研究報告書一份

處理方式：除產學合作研究計畫、提升產業技術及人才培育研究計畫、  
列管計畫及下列情形者外，得立即公開查詢

涉及專利或其他智慧財產權， 一年 二年後可公開查詢

執行單位：東海大學化工系

中華民國 95 年 10 月 31 日

中文摘要：

本研究利用丙烯酸丁酯與丙烯酸的共聚物為基材混合幾種有機蒙脫土製備奈米複材，並研究其流變行為以及結構受剪切流場的影響。從 X 光繞射以及 X 光小角散射測量中可以知道所製備的複材其蒙脫土多是層插型，也就是系酸鹽片以數片疊在一起。從流變的研究結果發現奈米複材之層插狀況與其線性黏彈性與剪切黏度有相當大的關連。光散射的實驗中可以得知：在不受力的狀況下，奈米複材中的蒙脫土片疊的擺置方向在空間中各向均等，在低剪切率下此各向均等的分佈方式基本上沒有改變。在高剪切率下則在流動的方向出現較強之散射，代表片疊出現配向的情況。當剪切行動停止後一分鐘內，此配向會漸消失，轉回未剪切前之各向均等的分佈方式但在較大角度的散射光強比未受剪切者較高，代表散射源的尺寸變小，亦即片疊所形成之散射源被剪切流場切碎。

。

關鍵詞：奈米複材，流變學，小角散射，蒙脫土。

Abstract:

This project employs poly(butyl acrylate-co-acrylic acid) as the matrix and five different organo-montmorillonites as the nano particle fillers to prepare nanocomposites and studies the rheological behavior of the composite melts and the structure evolution of the composite melts under shear flow. The results of X ray diffraction and small angle X ray scattering reveal that the four out of the five composites are of intercalated type, in which silicate layers of organo-montmorillonites arrange themselves in stacks of a few layers. The results of rheological measurements show that the gain in the  $d$  spacing in intercalation is strongly related to the linear viscoelasticity and shear viscosity of the composites. The results of light scattering show that the un-sheared melts are isotropic and when

subject to flow at low shear rates, the isotropy essentially preserves with an increases of light intensity at larger scattering angles. At higher shear rate, strong scattering occurs in the direction of flow indicating the orientation of the scattering centers. When shear is ceased, the isotropy restores with an increase in the intensity of scattering light at high angles comparing with the sample before shearing, indicating the breakup of the scattering centers.

Keywords: Nanocomposites, rheology, small angle scattering, montmorillonites.

前言：

在傳統的複合材料中，補強材的添加量通常都相當的大，最高加到 20% 才能提高機械性質到一定的程度，但在奈米複材的世界裡只要加入少量的蒙脫土，就能大量提高強度，但是提高強度的原因卻沒有被很明確的指出。一般複材的性質與其加工方式和填充料在基材中分佈的方式有很大的關係。本研究就是希望能夠藉由流變的方法與光學的方法進一步了解蒙脫土在聚合物融熔液中分佈及排列的形式、其產生的結構與流變性質之間的關係，且在施加流場下，期望能觀察到蒙脫土在聚合物融熔液中排列方式的轉變。

研究目的

本研究利用流變的方法研究片狀矽酸鹽/高分子之奈米複合材料。在不同的矽酸鹽濃度下，觀察流變行為的改變，並在剪切流場下以光散射的方法觀察複材融熔液中片狀矽酸鹽片結構在剪切場下演變的行為。

文獻探討

以片狀矽酸鹽加入高分子中製成奈米/高分子複合材料的研究至今已超過三十年，所使用的片狀矽酸鹽包括蒙脫土<sup>1-3</sup>、雲母片<sup>4</sup>、人造矽酸鹽片如Laponite<sup>5</sup>以及較大之黏土片如hectorite<sup>5</sup>等，所使用的高分子涵

蓋聚丙烯<sup>6,7</sup>、聚苯乙烯<sup>8,9</sup>、聚甲基丙烯酸甲酯<sup>10</sup>、polycaprolactone<sup>11</sup>、polyamide<sup>12</sup>、polyurethane<sup>13</sup>、epoxy<sup>14</sup>等。所製出的奈米複材可分為兩類：一為層插型，即矽酸鹽仍維持層狀結構，只是高分子進入矽酸鹽之層間使層間距增加。另一則是剝離型，矽酸鹽片以單片的形式懸浮在聚合物中。

截至目前為止，學界對奈米矽酸鹽複材的流變性質的研究介入較少，其熔融液在靜態或流動狀態的結構研究更少。對於層插型的系統而言，現有的剪切黏度研究結果有些分歧，不同的系統有相異的行為，如Krishnamoorti等人<sup>15</sup>發現poly(methylsiloxane-co-diphenylsiloxane)與蒙脫土所製成的複材在低剪切率時表現出牛頓流體的特徵，高剪切率時則顯現剪稀；隨著矽酸鹽的增加，複材的黏度增加且剪稀的臨界剪切率降低。和這個結果類似的有Hyun等人<sup>16</sup>研究之聚乙烯氧/蒙脫土系統的黏度，但此系統的臨界剪切率較高，大約落在 $0.06\text{s}^{-1}$ 至 $1.0\text{s}^{-1}$ 之間。Solomon等人<sup>17</sup>所發表的聚丙烯/蒙脫土系統就不太一樣，他們發現在整個 $0.001\text{s}^{-1}$ 至 $1\text{s}^{-1}$ 的範圍內黏度均呈現剪稀現象，且隨著蒙脫土含量的增加剪稀的現象越嚴重。與這結果類似的系統有Ren等人<sup>18</sup>所發表的poly(styrene)-poly(isoprene)共聚物/蒙脫土系統。而楊怡寬等人<sup>19</sup>所發表的poly(butyl methacrylate)/蒙脫土系統與胡啟正<sup>20</sup>所研究的聚苯乙烯/蒙脫土系統則是都發現在低蒙脫土含量在較低剪切率下出現牛頓流體行為，在高蒙脫土含量則仍是整個剪切率範圍都呈現剪稀現象。

在奈米矽酸鹽複材的線性黏彈性質的研究方面，關於層插型的系統有不少的文獻報告如蒙脫土與聚丙烯<sup>7</sup>、聚苯乙烯<sup>20</sup>、耐龍<sup>6</sup><sup>11</sup>、聚乙烯氧、poly(styrene)-poly(isoprene)<sup>21</sup>、poly(butyl methacrylate)<sup>19</sup>、polycaprolactone<sup>11</sup>等聚合物製成之複材。各文獻所得線性黏彈性結果相當一致。主要結論如下：

- (1)  $G'$ 與 $G''$ 均隨著矽酸鹽的含量增加而增加，但在低頻率時的增加效果遠高於高頻率時。
- (2)  $G'$ 與 $G''$ 在高頻率的行為與高分子主體

差異不大。

- (3)  $G'$ 與 $G''$ 隨著矽酸鹽片之濃度增加在低頻率的範圍中顯現出異於一般無填充物之高分子的非典型終端行為。此低頻終端斜率在濃度大於一個臨界值時斜率幾乎為零，而且濃度再繼續增加，終端斜率也不再降低。
- (4) 大部分的 $G'$ 與 $G''$ 均服從溫度-時間重疊原則(time-temperature superposition principle)。其頻率校正因子 $a_T$ 均遵循Arrhenius律，且其活化能與並與聚合物的本體者一樣。

目前多數的研究者對於奈米複材之流變行為的解釋各有不同；Galgali等人<sup>7</sup>認為此似固行為與矽酸鹽片間的摩擦有關，而少數的剝離矽酸鹽片會將沒剝離的層插片集連結形成網狀結構抵抗變形。大多數的研究者認同Ren等人<sup>18</sup>的看法，他們都認為低剪切率的剪稀行為以及 $G'$ 的非典型終端行為是另一個似固結構的表現。此似固的結構是由幾片到幾十片的矽酸鹽疊成一個片疊(tactoid)。而聚合物分子在此片疊附近的範圍產生局部的有序的區塊，就如同液晶的疇(domain)<sup>22</sup>。在疇之間形成的晶界乃是較高自由能的區域，也是產生似固結構的來源。此似固結構會隨剪切強度增加漸次瓦解。

## 研究方法

先利用自由基聚合的方法合成出含3%壓克力酸-丁基丙烯酸酯隨機共聚高分子(以AA-co-BA簡稱)作為基材。為了挑選能與上述基材形成良好的複材的片狀片本研究將五種有機蒙脫土(Cloiste 25A、30B、APA、93A、NanomerI34)以溶液層插法與基材製備成5%濃度的複合材料，然後將複合材料經由X-ray繞射(XRD)測量蒙脫土之層間距變化，以檢視視片狀矽酸鹽片在聚合物中的分散狀況；此外，也對製備完成的複材融熔液使用旋轉式流變儀(RDAII)，以動態模式頻率掃描，取得在 $50^\circ\text{C}$ 下複合材料的基本流變數據作為選擇蒙脫土的依據。經過篩選後本計畫取Cloiste 25A作為研究的對象系統，並製備各種不同濃度Cloiste 25A的複

材，以供研究觀察。對這些不同濃度的複材本研究使用旋轉式流變儀(RDAII)，以動態模式頻率掃描，在不同溫度下取得其線性黏彈性的數據；並在暫態模式下找出不同剪切速率、不同溫度跟不同濃度時，複合材料的黏度達穩定之時間，再以穩態模式速率掃描測出不同剪切速率下之穩態黏度，用於推測穩態下複材流體的蒙脫土結構的轉變。藉著旋轉式流變儀的所得之結果，在剪切加熱平台以加上光散射的技術，觀察在剪切過程中，散射圖形的變化。將光散射的散射圖與流變數據作對照與比較。

### 結果與討論

從大角度XRD結果(表 1)可以看出所製備的複材中僅有含 30B的複材是剝離型的，而其餘的複材均呈現層插型。比較層插型的複材可以發現的層間距的按大小順序排列是 I34>APA >25A>93A。所有的複材的XRD圖上均可以看見一個較弱的峰，且此峰的位置與複材所含之蒙脫土未與基材混練前呈現之XRD峰十分接近，這表示每個複材都含有少量未撐開或被壓縮的蒙脫土。在小角X-ray散射圖(圖 1)中可以發現下含I34 及APA在 $Q=0.16\text{\AA}^{-1}$ 處有一個分佈叫寬的峰而含 25A的複材則在 $Q=0.23\text{\AA}^{-1}$ 處有一個很弱的峰，含 93A與 30B的複材則不見有干涉峰的存在。這結果大致與XRD的結果相符。在 $50^\circ\text{C}$ 下以流變儀所得的線性黏彈性資料顯示(圖 2 與圖 3)，除了含 93A之複材融熔液行為較特殊外  $G'$  與 $G''$ 之值在所測的頻率範圍內以所含的黏土做標示可以用下列的順序表示APA>I34>25A>30B，此順序中之前四個層插型複材的順序與XRD所得之層間距順序十分接近。含 93A之複材融熔液其 $G'$ 值在高頻時是所有複材中最低的，在中低頻率時卻比含 25A的複材高，在更低頻時甚至高過含I34者；其 $G''$ 值也是最低的，但在低頻時卻高過含 25A的複材。在低頻率時，複材之 $G'$ 的斜率均較基材為低，而以含I34者最為明顯甚至有呈現其曲線水平之跡象，在文獻上此低頻斜率的拉平表示有固態結構的產生。含 30B之複材雖是剝離型的蒙

脫土呈現方式，卻沒有較高的黏彈性值，由此可說蒙脫土的剝離並不一定能有效提升性質，這可能與此矽酸鹽改質的介面活性劑與基材高分子之間的作用力薄弱有關。

接下來的研究來我們選定AA-co-BA/25A的系統。在XRD圖(圖 3)中可以看到：與純25A比較起來，含 25A的複材其繞射峰向小角度的方向位移，同時也產生另一個繞射峰向大角度的方向移動，這似乎暗示著有小部分的蒙脫土其層間距是被縮小的；這與小角X光散射中(圖 1)在對應的位置上發現弱峰訊號相符，我們判斷此複材仍然是屬層插型且原黏土之層間距被撐大了。我們在RDAII所測得之的黏彈性結果中發現當固定溫度時，矽酸鹽的濃度上升會使 $G'$ 與 $G''$ 提高，且含量在 1%至 3%時有明顯的增加，相對含量在 3%至 7%時增加的幅度就沒這麼大(圖 5 與圖 6)。當固定濃度時，溫度提高 $G'$ 與 $G''$ 會下降，且從 $30^\circ\text{C}$ - $40^\circ\text{C}$ 時下降的特別明顯(圖 7 與圖 8)，濃度較高時溫度上升，低頻斜率會慢慢拉平，表示可能複材之結構會隨溫度而改變。在暫態實驗中剪切速率越快達穩態時間越短，但在剪切率較高時會有因邊緣破裂(edge fracture)導致流料的情況發生而無法測得穩態黏度。為了避免流料的問題發生，在穩態實驗時夾具改以平板-杯型，改以這種方法會使得測得黏度時稍微偏大，但可以避免流料的問題。在實驗結果中發現，在含量為 1%的複材在低剪切速率呈現出牛頓流體的行為，大約在剪切率超過 $9\text{s}^{-1}$ 後出現剪切稀的情況。蒙脫土含量在 3%以上之複材則沒有牛頓流體的行為；整個探討的剪切率範圍內可以區分為兩個剪切稀區：第一個區為弱剪切稀區發生在較低剪切率的範圍內，第二個區為強剪切稀區在較高的剪切率範圍。矽酸鹽濃度越高的情況下，切稀的程度越嚴重，且由弱剪切稀區轉成強剪切區的剪切速率越低(圖 9)。但隨著溫度的上昇，黏度值會下降會使得 1%的複材出現牛頓流體的行為的範圍延後到較高的剪切速率如 $10(1/\text{s})$ (圖 10)。在所有的剪切黏度取現中強剪切區都有黏度在某個特定的剪切率突然增加的現象且此特定之剪切率隨

溫度增加而增加。導致這現象的原因不明仍待探討。在剪切黏度 $\eta$ 與複數黏度 $\eta^*$ 之比較(圖 11 與 12)中發現,在低剪切率下 $\eta$ 值稍大於 $\eta^*$ 值,而超過某個剪切率後 $\eta^*$ 大於 $\eta$ 。由於本黏度測量使用平行板夾具,所測得之剪切黏度為表觀黏度,未經修正前是比實際剪切黏度值稍高。在低剪切率下修正後的剪切黏度應會接近於複數黏度,而高剪切率下修正後之剪切黏度與複數黏度之差會比原先表觀黏度與複數黏度之差還要嚴重。一般而言, $\eta^*$ 是由動態頻率掃描的 $G'$ 與 $G''$ 計算出來的,由於動態頻率掃描的測量中震幅極低,所以,對材料結構不會有破壞,而單方向剪切則對結構會造成相當大的破壞。究其原因可能是在固定溫度下,低頻下之複數黏度與低剪切率下之剪切黏度接近相同表示兩者結構在剪切下並無不同;高頻之複數黏大於高剪切率下剪切黏度且兩者之差隨剪切率(頻率)增加而變大代表超過特定剪切率後單向剪切造成結構變化而且剪切率越高下所形成之結構其與原始結構差異越大。從圖 13a、b及c的光散射圖可以得知:在低剪切率下光散射基本上是各向均等的,也就是沒有配向的出現。隨著剪切率的增加在高角度的光散射的強度增加代表散射原有被切成較小尺寸的傾向,又隨著剪切率的繼續增加可以發現光散射在流動方向增強而其他方向減弱,這代表配向發生,暗示著由蒙脫土之矽酸鹽片所構成之結構有在流動方向產生配向。這樣的結構變化與穩態剪切黏度的兩個不同的剪切稀行為吻合。高剪切率下之配向在停止剪切後約一分鐘內,光散射圖又變成各向均等代表配向的消失(圖 13d)。這說明此結構的配向在剪切時是一種結構而此結構甚易被還原成等向之結構,這可能與系統的正向力有關。

## 結論

對丙烯酸丁酯與丙烯酸的共聚物為基材製成之有機蒙脫土奈米複合材料而言,其複材之矽酸鹽片與基材所形成之結構與有機蒙脫土之界面活性劑有很大的關連。此系統之奈米複材融熔液之線性黏彈性質與複

材之結構息息相關。此系統之高濃度層插型複材在線性黏彈性之儲存模數以及消耗模數均表現出異常之低頻終端行為;其複數黏度也在低頻與高頻分別出現兩段不同之剪切稀行為。穩態剪切黏度也在低與高剪切率區域也分別出現兩段不同之剪切稀行為。與複數黏度相比較,兩者在低剪切率或低頻率下之行為類似,但在高剪切率或高頻下穩態剪切黏度低於複數黏度。從光散射的結果得知隨著剪切率的增加,穩態剪切會切碎複材結構,再使結構產生配向,這可以解釋穩態黏度的兩段切稀行為。

## 參考文獻

1. G. Chen, S. Liu, S. Zhang and Z. Qi, *Macromol. Rapid Commun.*, **21**, 746 (2001).
2. T. H. Kim, L. W. Jang, D. C. Lee, H. J. Choi and M. John, *Macromol. Rapid Commun.*, **23**, 191 (2002).
3. P. Aranda and E. Ruiz-Hitzky, *Chem. Mater.*, **4**, 1395 (1992).
4. S. D. Burnside and E. P. Giannelis, *Chem. Mater.*, **6**, 1017 (1995).
5. C. A. Mitchell and R. Krishnamoorti, *J. Polym. Sci. Polym. Phys.* **40**, 1434 (2002).
6. P. Reichert, B. Hoffmann, T. Bock, R. Thomann, R. Mulhaupt and C. Friedrich, *Macromol. Rapid Commun.*, **22**, 519 (2001).
7. G. Galgali, C. Ramesh and A. Lele, *Macromolecules*, **34**, 852 (2001).
8. B. Hoffmann, T. Bock, R. Thomann, C. Friedrich and R. Mulhaupt, *Macromol. Rapid Commun.*, **22**, 519 (2001).
9. Y. T. Lim and O. O. Park, *Macromol. Rapid Commun.*, **21**, 231 (2000).
10. X. Hu, W. Zhang, M. Si, M. Gelfer, B. Hsiao, M. Rafailovich, J. Sokolov, V. Zaitsev and S. Schwarz, *Macromolecules*, **36**, 823 (2003).
11. R. Krishnamoorti and E. P. Giannelis, *Macromolecules*, **30**, 4097 (1997).
12. K. Yano, T. Karauchi and O. Kamigaito, *J. Polym. Sci. Polym. Chem.*, **31**, 2493 (1993).

13. T. K. Chen, Y. L. Tien and K. H. Wei, *J. Polym. Sci. Polym. Phys.*, **37**, 2225(1999).
14. N. Salahuddin, A. Moet, A. Hiltner and E. Baer, *Euro. Polym. J.*, **38**, 1477(2002)
15. E. P. Giannelis, R. Krishnamoorti and E. Manias, *Adv. In Polym. Sci.* V138, Springer-Verlag Berlin Heidelberg (1999)
16. Y. H. Hyun, S. T. Lim, H. J. Choi and M. S. Jhon, *Macromolecules*, **34**, 8084(2001)
17. M. J. Solomon, A. S. Aalmusallam, K. F. Seefeldt, A. Somwanhanaroj and P. Veradan, *Macromolecules*, **34**, 1864(2001)
18. J. Ren, A. S. Silva and R. Krishnamoorti, *Macromolecules*, **33**, 3739(2000).
19. I. K. Yang and C. C. Hu, *Euro. Polym. J.* (2006)
20. 胡啟正，碩士論文，東海大學化學工程學系 2003 年 7 月。
21. R. Krishnamoorti, J. Ren and A. S. Silva, *J. Chem. Phys.*, **114**, 4968(2001).
22. T. S. Asada, S. Onogi and H. Yanase, *Polym. Eng. Sci.*, **24**, 355 (1984).

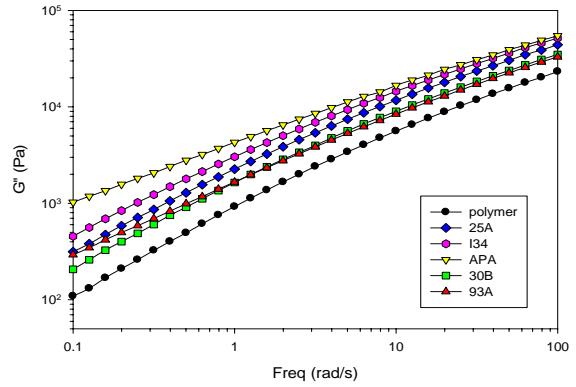


圖 3、50°C 下各種複材頻率掃描 G' 比較圖

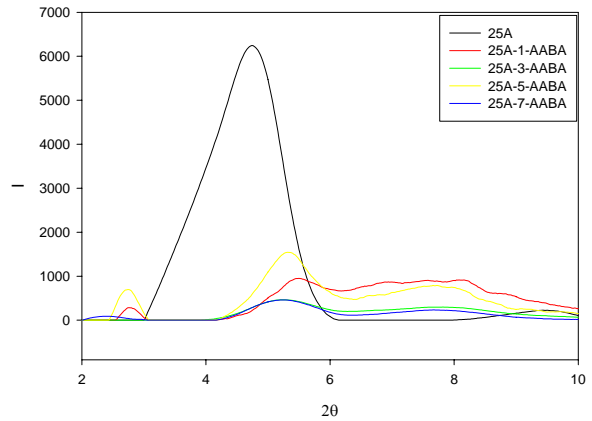


圖 4、25A 含量為 1,3,5,7% 之複材的 XRD 圖。

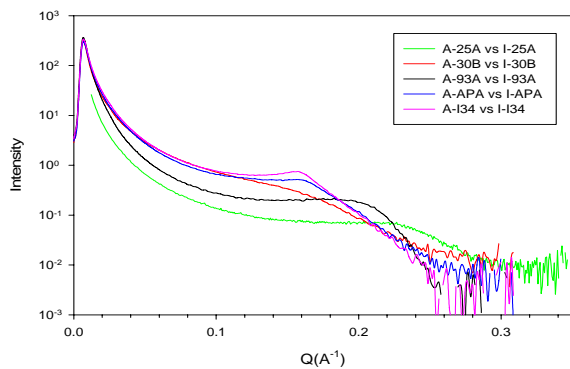


圖 1、不同蒙脫土複材之小角光散射圖。

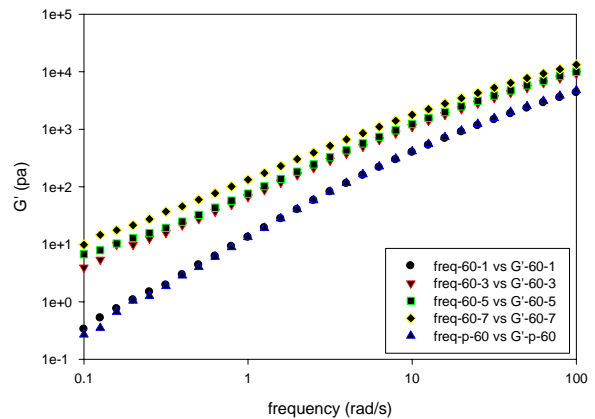


圖 5、60°C 各濃度複材 G' 之頻率掃描圖。

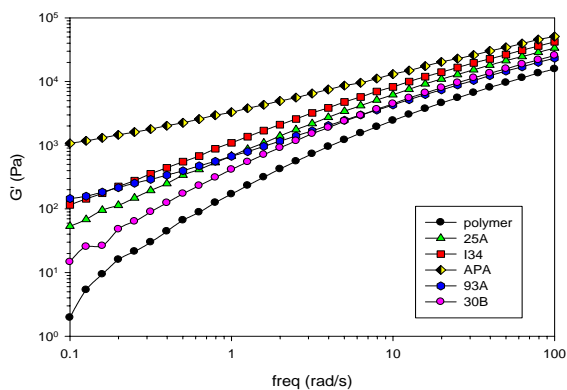


圖 2、50°C 下各種複材頻率掃描 G' 比較圖。

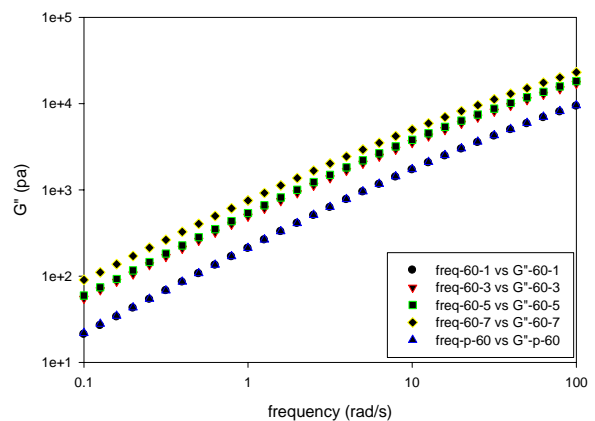


圖 6、60°C 下各濃度複材之 G'' 頻率掃描圖。

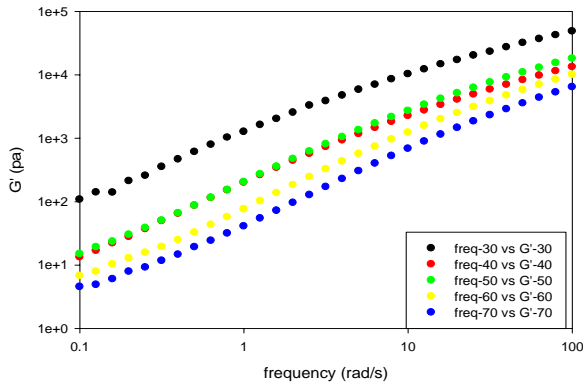


圖 7、濃度 5% 時各溫度下之  $G'$  頻率掃描圖。

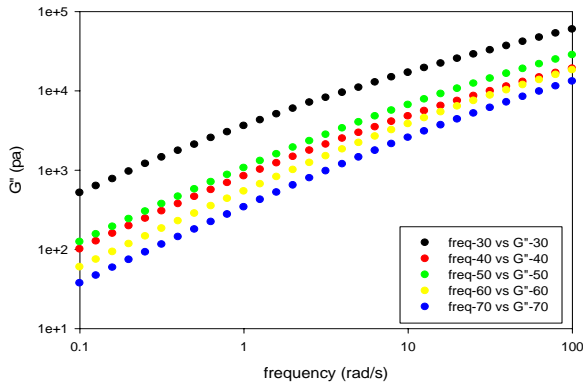


圖 8、濃度 5% 時各溫度下之  $G''$  頻率掃描圖。

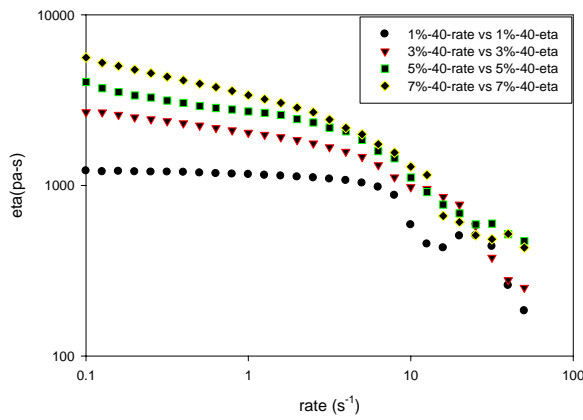


圖 9、 $40^{\circ}\text{C}$  下不同濃度複材之剪切黏度圖。

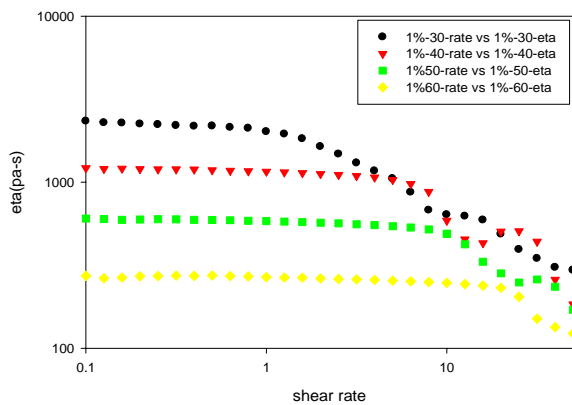


圖 10、1% 濃度之複材在不同溫度下剪切黏度圖。

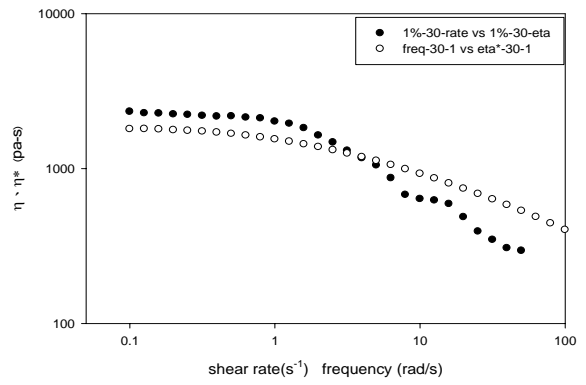


圖 11、1% 濃度之複材之複數黏度與剪切黏度比較圖。

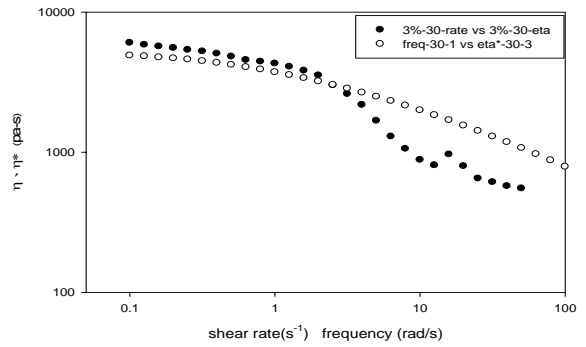


圖 12、3% 濃度之複材之複數黏度與剪切黏度比較圖。



圖 13a、含 25A 7% 之複材在剪切率為  $2\text{s}^{-1}$  光散射圖。

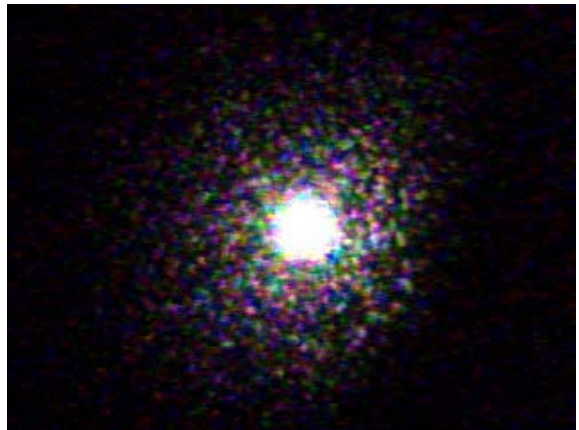


圖 13b、含 25A 7% 之複材在剪切率為  $10\text{s}^{-1}$  光散射圖。



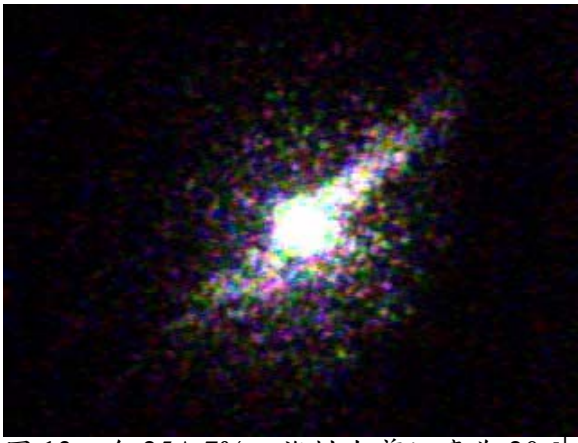


圖 13c、含 25A 7%之複材在剪切率為  $20\text{s}^{-1}$  光  
散射圖。



圖 13d、含 25A 7%之複材以停止剪切率為  
 $20\text{s}^{-1}$  之剪切後一分鐘之光散射圖。

表一、複材特徵峰比較表

	低角繞射峰	中角繞射峰	高角繞射峰
	$2\theta$ (層間距 Å)	$2\theta$ (層間距 Å)	$2\theta$ (層間距 Å)
蒙脫土 I34			4.52(19.55)
複材 5% I34	2.12(41.67)		4.58(19.30)
蒙脫土 APA	2.84(31.11)		4.72(18.72)
複材 5% APA	2.64(33.46)	3.36(26.29)	4.60(19.20)
蒙脫土 25A			4.74(18.64)
複材 5% 25A	2.74(32.24)		5.32(16.99)
蒙脫土 93A		3.82(23.13)	
複材 5% 93A	3.0(29.45)		
蒙脫土 30B			4.94(17.98)
複材 5% 30B	None	None	None

## 參加國際學術會議心得報告

2005/09/03

會議名稱：4<sup>th</sup> Pacific Rim Conference on Rheology (PRCR4)

會議地點：中國上海

會議期間：94/08/07-94/08/11

報告者：蔡秉宏

很榮幸能參加在中國上海由中國化學學會流變學專業委員會、中國力學學會流變學專業委員會舉辦的第四屆亞太地區流變學國際會議，並提出口頭報告。此次大會主題包含複雜流體的模擬與構成理論、流變學與新技術、聚合物與多相熔融體、非牛頓流體力學與計算流變學、固體與複材流變學、電-磁流變學與高科技材料、岩石-土壤流變學、高分子溶液及膠體及天然與生物材料流變學等，內容幾乎包含了整個流變學的領域。

會議開始的第一天上午，由 Dr. Mckinley 進行「Extensional Flows of Polymer Solutions in Microfluid Converging/Diverging Geometries」的專題報告。在他的演講中提及了有關非牛頓流體在微流體縮小/放大幾何形態中流體彈性的影響。他們發現流體結構的形狀、大小與發展與彈性數 ( $El = \eta\lambda / \rho L \left( \frac{1}{D_2} - \frac{1}{D_1} \right)$ ) 相依，這個彈性數與流動的動力無關只與流體的性質與流道的特徵尺寸相依。這方面的研究與噴墨印刷的應用有關。在每個物件力求微型化的將來，這個領域的研究對裝置的設計很重要，也是很值得進一步探討的研究主題。之後，大會還安排多場的專題演講，且在場外並有論文海報的展示。

會議第二天，仍繼續進行論文報告，包括複雜流體的模擬與構成理論、流變學與新技術、聚合物與多相熔融體、非牛頓流體力學與計算流變學等領域。

會議第三天仍有相當多有趣的論文主題發表，我的指導教授楊怡寬於上午的 Polymer & Multi-phase Melts 場次進行論文口頭報告，報告的論文題目是「Rheological Characterization and Microphase Separated Structure of a Poly(ether-block-amide) Segmented Block Copolymer」，報告時間為 20 分鐘，討論 5 分鐘，進行口頭報告相當順利，且與參與的學者有都熱烈參與並提出問題，在交流中，使我獲益不少，並得到相當多的建議。

會議的最後一天進行了電-磁流變學與高科技材料、岩石-土壤流

變學、高分子溶液及膠體及天然與生物材料流變學等主題的相關論文發表。在這些天的會議中，我參加了許多場次的演講，並且吸收了相當多的知識並且對現今流變學的進展有更深刻的認識。

整體而言，這是一次成功而多元的國際學術會議，此次參加會議，深深感受到高分子流變學在高分子加工中的重要性並體驗到外國學者研究的深度與紮實，也對上海地區繁榮景象與人們的熱情留下深刻印象，對自己在未來研究與論文的發表上，也有更多的刺激與幫助。

## Rheology and Structure Change of a Poly(ether-block-amide) Segmented Block Copolymer

I-Kuan Yang<sup>1,a</sup>, Ping-Hung Tsai<sup>1,b</sup>

<sup>1</sup> Department of Chemical Engineering, Tunghai University Taichung, Taiwan, ROC,

<sup>a</sup> ikyang@mail.thu.edu.tw, <sup>b</sup> d903102@student.thu.edu.tw

**Keywords:** poly(ether-block-amide), rheology, infrared spectrum, microphase separation, hydrogen bonding, atomic force microscopy.

**Abstract.** Melt of a segmented block copolymer constituting of poly (lauryl lactam) as the hard segment and poly (tetramethylene oxide) as the soft segment was investigated by rheological techniques. Storage modulus of the polymer melt exhibits the non-terminal behavior resembling those of diblock and triblock copolymer melts, indicating the existence of a microphase separated structure. Contrarily to most block copolymers, the melt of the segmented block copolymer transforms from a weak structure to a stiff one upon raising temperature. Atomic force microscopic data in tapping mode reveals that at low temperatures the structure of the melt is constituted of small spherical soft domains dispersed in a hard matrix and the hardness of the matrix differs slightly from that of the domains; at high temperatures the spherical domain structure preserves but the domain becomes larger and so does the hardness difference between the domain and the matrix. Infrared spectrum analysis shows that the temperature induced structural change is related to the dissociation of hydrogen bonding between the hard and the soft segments.

### Introduction

Thermoplastic elastomers (TPEs) are block copolymers composed of thermodynamically incompatible blocks, and frequently exhibit a microphase-separated morphology [1,2]. Segmented block copolymer is a sub-category of TPEs with multi-alternating blocks which can be expressed by a general formula  $(-A-B-)_n$ , and the molar mass of each segment is usually lower than 4,000 [1]. Polyurethane, poly (ether-ester), and poly (ether-block-amide) (PEBA) belong to this category. PEBA consists of an aliphatic polyamide as the hard block and a polyether as the soft block and between the two blocks a di-acid serves as the joint. PEBA shows microphase separation due to the great polarity difference between the hard and the soft segment [3].

Various tools including differential scanning calorimeter [2, 4], dynamic mechanical analysis [2, 5], thermally stimulated current method [6], dielectric analysis [7], wide angle X-ray diffraction [2], small angle X-ray scattering [8], transmission electron microscopy [5], and atomic force microscopy [9] had been used to investigate the thermal and the phase behavior of PEBA. Most of the investigations [4,9] showed consistent results that the polymer exhibited a separated multiphase morphology that included a well-defined polyamide crystalline phase, a polyamide amorphous phase, and a polyether amorphous phase. These phases were arranged in periodical planar alternating layers [12].

PEBA has been commercialized for at least a decade, studies on the properties in solid state are abundant, but the information about the rheology and the structure of the polymer in the molten state is still insufficient. The present work concentrates on the rheological behavior and the structure of PEBA melts. We used rheological techniques to study the structure of a polyether-block-amide. The polymer was found exhibiting an abnormal terminal behavior and opposite to that of diblock and triblock polymers, the polymer melt transformed from a weak structure to a stiff structure upon temperature increasing. Consistent with the rheological observations, the results of tapping mode AFM showed that the domains of the soft segments of the polymer melt coarsened, and the hardness difference between the domain and the continuous matrix enlarged as temperature increased. Analysis of the infrared spectra showed that the structure change could be related to the dissociation of hydrogen bonding.

### Experimental

**Materials.** The PEBA used in this work was a commercial product of Elf Atochem Inc and its trade name is Pebax 5533. The hard segment of PEBA is poly(lauryl lactam) (PA 12) and the soft segment is poly(tetramethylene oxide) (PTMO), and adipic acid is the linkage. The average molecular weight of the polymer is reported at about 50000[13]. The molecular structure of the PEBA was obtained by <sup>1</sup>H NMR spectra with a Bruker AMX-400 spectrometer. Element analysis (Heraeus CHNOS Rapid F002) was also used to determine the composition of the polymer.

**Sample Preparation.** To prepare the samples for rheological measurements, powder of the PEBA was placed in a vacuum oven at 80°C for 24 hours to remove moisture. The moisture free samples were sandwiched between Teflon sheets and heated and kept at 185°C for about 5 minutes before thermo-pressed into films of 1.2 mm thickness at the same temperature.

**Rheological Measurements.** Linear viscoelastic properties were measured under nitrogen atmosphere on a rotational type rheometer (RDA II, Rheometrics Co.) using a parallel plate fixture with a gap of 0.8-1.0 mm and a diameter of 40 mm. All measurements were performed at 2% strain. The time range for thermal stability of PEBA at the testing conditions was determined by monitoring the change of modulus  $G'$  and  $G''$  and all rheological measurements were completed within the time limits of thermal stability. The data reported in this work were the average of at least five different measurements.

**Fourier Transform Infrared Thermal Analysis.** The infrared spectra of the PEBA were performed at a resolution of  $2\text{ cm}^{-1}$  on IR Prestige-21 (Shimadzu Inc.) equipped with a high temperature transmission cell (Model HT-32, Spectra-Tech Inc.) connected to a temperature/process controller (CN325, Omega Technologies Inc.). Thermo-pressed sample film of  $15\ \mu\text{m}$  thickness was inserted into the cell. In each measurement a minimum of 64 scans was taken and then averaged. The temperature accuracy was within  $\pm 1^\circ\text{C}$ . PeakFit version 4.1 developed by SYSTAT Software Inc. was adopted to do the de-convolutions of FTIR spectra.

**Atomic Force Microscopy.** Atomic force microscopy was conducted in tapping mode on a SPI3800N SPA-400 (Seiko Instruments Inc). The films for the microscopy were obtained by spreading a 10 wt % solution of hexafluoro-2-propanol (HFIP) onto glass microscope slides; then the films were dried in a hood for several minutes at room temperature before being placed in a vacuum oven at  $80^\circ\text{C}$  for 7 days to remove residual solvent. In order to freeze the morphology of the PEBA in the molten state, the cast film was placed in an oven at a prescribed temperature for at least 10 minutes before being quenched by liquid nitrogen.

## Results and Discussion

The dynamic modulus spectra of the PEBA are shown in Fig. 1. For each isotherm, the loss modulus  $G''$  of the PEBA shows a monotonic decrease with the decrease in frequency. On the same figure it can be seen that similar to most polymer melts, both  $G'$  and  $G''$  decrease as temperature increases and a small drop occurs between  $180^\circ\text{C}$  and  $190^\circ\text{C}$ . All isothermal curves of  $G''$  tend to be parallel to each other at low frequencies with a slope close to 1.0, which is the normal terminal slope for homo-polymer melts. The storage modulus  $G'$  of the PEBA behaves distinctly at different temperatures. Following the  $170^\circ\text{C}$  isothermal curve, one can easily see that  $G'$  monotonically decreases as the frequency decreases over the range of frequency investigated. At temperatures higher than  $170^\circ\text{C}$ ,  $G'$  collected at higher frequencies essentially preserves the same monotonic decreasing trend as that at  $170^\circ\text{C}$ , but the decrease decelerates when a critical frequency is surpassed. As the temperature is raised to  $200^\circ\text{C}$  and beyond, a level off of  $G'$  at low frequencies can be clearly seen. For a homogenous polymer melt, the expected normal terminal behavior is that as the frequency  $\omega$  approaches very small values, the proportionalities that  $G' \propto \omega^2$  and  $G'' \propto \omega$ . The storage modulus of the segmented copolymer obviously does not follow the normal terminal behavior. Change of terminal behavior over the temperature range implies that the segmented copolymer undergoes a structure transition.

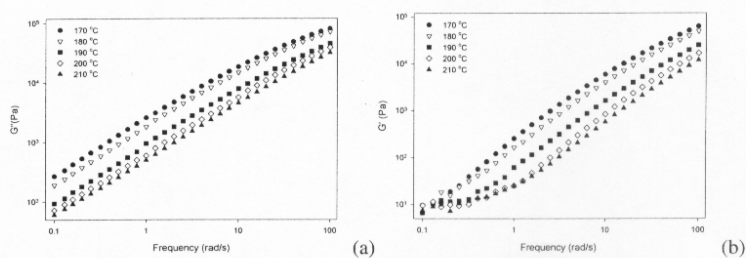


Fig.1. The loss and the storage modulus of Pebax 5533 melt. (a)  $G''$ , (b)  $G'$ .

Shown in Fig. 2 are atomic force microscopic data of the film surface of the PEBA quenched from melts at  $170^\circ\text{C}$ ,  $190^\circ\text{C}$  and  $210^\circ\text{C}$  respectively. For the phase lag data of a tapping mode the gray level is related to the hardness of the probed region and a darker color indicates the region probed is softer. It is known that the hard segment of the PEBA is composed of polyamide, thus the gray level in the microscopy reflects the content of the hard segment in the probed region and the lighter region is richer in hard segment and vice versa. Contrarily to the previous reports that PEBA assumed a lamellar morphology at room temperature, a spherical microdomain structure was found for the PEBA melt. In all three microscopic pictures, spherical dark domains with different gray levels are randomly distributed over the entire scan box, and for the film quenched from low temperatures, e.g. from  $170^\circ\text{C}$ , the size of domains is quite uniform and the difference between the gray level of the spherical domain and that of the continuous matrix is small making the overall picture more homogeneous in gray level than the other two. The domain size grows from 30 nm to about 100 nm as the temperature of the melt increases from  $170^\circ\text{C}$  to  $210^\circ\text{C}$  and

simultaneously, the raise of the temperature enlarges the contrast between the dark and light region, or the matrix becomes much brighter and the spherical domains becomes strictly dark. The growth of the domain size and the enlargement of the contrast between the spherical domain and the matrix indicate the demixing of the hard segment and the soft segment in the PEBA melts as the temperature rises. Though, it was reported that PEBA shows microphase separation [9] due to the polarity difference between the hard and the soft segment, PEBA may resemble polyurethane [11] showing limited compatibility between the two segments due to the hydrogen bonding that links the NH group in hard segments to the ether group and the carbonyl group of the ester in soft segments. The change and the destruction of hydrogen bonding with increasing temperature may therefore be the driving force for the demixing of the hard and the soft segment.

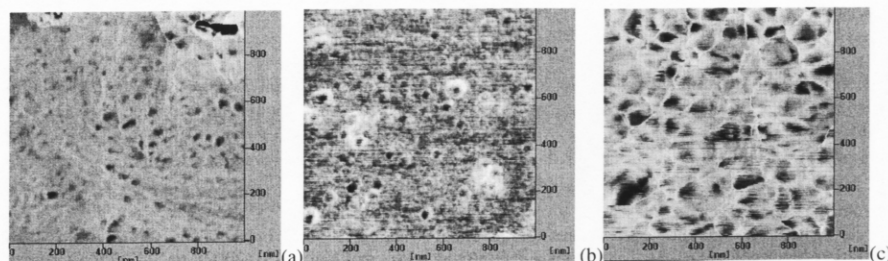


Fig.2. AFM phase data for Pebax 5533 film surface quenched from 170°C(a), 190°C(b) and 210°C(c).

The triggering of structure change upon temperature raise reminds us of hydrogen bonding, for the reason that entropy-origin incompatibility between polymers can be relieved by the compensation of the strong intermolecular interaction such as hydrogen bonding. Contrarily, losing hydrogen bonding upon raising temperature induces demixing of polymers. In order to understand the temperature dependence of the hydrogen bonding and the relationship between the hydrogen bonding and the microphase structure, we used Fourier transform infrared thermal analysis to characterize the evolution of hydrogen bonding upon raising temperature.

In the present work, we focus on the area changes of the stretch band of hydrogen-bonded carbonyl groups and free carbonyl groups. The absorption band of the ester carbonyl group stretch mode covers an interval of wave number ranging from 1710 to 1800  $\text{cm}^{-1}$ . Two absorption bands are found overlapped in this range; one centers around 1737  $\text{cm}^{-1}$ , which is the absorption band of the hydrogen-bonded carbonyl, while the other centers at 1770  $\text{cm}^{-1}$  representing that of the ester carbonyl and this band appears as a tail attached to the former. From Fig. 3(a) it can easily be seen that as the temperature rises, the absorption band of the ester carbonyl broadens and the peak shifts toward higher wave number, and in the mean time, the tail grows. Through curve fitting, we obtain the areas representing a quantitative measure of the amount of these two components at various temperatures. From Fig. 3(b) One can easily see that the area fraction of the hydrogen bonded carbonyl decreases with increasing temperature and a sudden drop occurs at 160-170 °C. Between 170 and 180 °C the fraction remains constant until another drop starts. The free carbonyl behaves exactly opposite to the bonded carbonyl. Weakening and dissociation of hydrogen bond with rising temperature explains the decrease of area fraction for bonded carbonyl over the temperature range below the melting point. The drop at 160°C simply reflects the melting of the hard segments, but the second drop could imply a transition of the structure within this temperature range which is consistent with the results of the rheological characterization and suggests the formation of the stiffer structure upon the temperature raise is associated with the dissociation of hydrogen bonding that demixing the soft and hard segments. We are convinced that shortly after melting, the PEBA melt obtains a liquid like microphase separated structure exhibiting a terminal slope of 1.6 for storage modulus and the further dissociation of the hydrogen bonding results in a stiffer microphase separation structure accompany with an abnormal terminal behavior.

### Summary

Rheological techniques and Fourier transform infrared thermal analysis were applied to characterize the properties and structure of a poly(ether-block-amide) segmented copolymer. Studies of linear viscoelasticity suggest that the microphase-separated PEBA melt transforms from a weak structure to a stiff structure as temperature rises. AFM reveals that the weak structure at temperatures just above the melting point of polyamide crystallite has a nearly homogeneous microphase separated structure with small spherical domains, and the stiff structure at higher temperatures contains coarser spherical domains in which the composition is more distinctively different from that in the matrix. Hydrogen bonding between the soft and the hard segment is responsible to the transformation of the structure. With increasing temperature, hydrogen bonding dissociates to demix the soft and hard segment mixture and the polymer assumes a stiff microphase-separated structure, which reflects the change of the linear viscoelasticity and morphology.

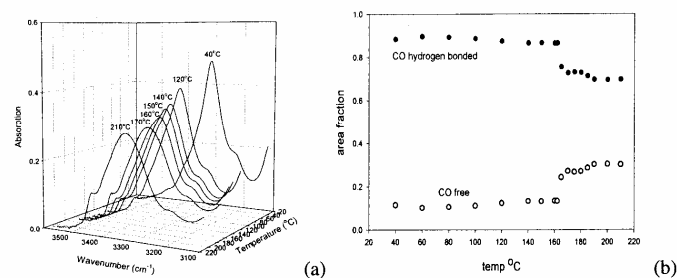


Fig.3. (a) FTIR spectra of ester carbonyl of Pebax 5533 melts at different temperatures. (b) Temperature dependence of the IR absorption area fractions of hydrogen-bonded ester carbonyl and free ester carbonyl.

### References

- [1] N.R. Legge. Thermoplastic elastomers - A Comprehensive review, Carl Hanser Verlag, Kolbergerstr, New York 1987.
- [2] J.P. Sheth, J. Xu and G.L. Wilkes. Solid state structure-property behavior of semicrystalline poly (ether-block-amide) PEBAX thermoplastic elastomers. *Polymer* Vol. 44(3) (2002), pp. 743-756.
- [3] P. Maj and D. Cuzin. Block polyamide-polyester preparation, (Atochem, Fr.). F.R. Patent 2,672,053, September 24, 1992.
- [4] M.L. Di Lorenzo, M. Pyda and B. Wunderlich. Calorimetry of nanophase-separated poly (oligoamide-alt-oligoether)s. *Journal of Polymer Science, Part B, Polymer Physics* Vol. 39(14) (2001), pp. 1594-1604.
- [5] M. Xie and Y. Camberlin. Morphological study of block copoly(ether-amide)s. *Makromolekulare Chemie* Vol. 187(2) (1986), pp. 383-400.
- [6] H. S. Faruque and C. Lacabanne. Study of multiple relaxations in pebax, polyether block amide (pa12 2135 block ptmg 2032), copolymer using the thermally stimulated current method. *Polymer* Vol. 27(4) (1986), pp. 527-531.
- [7] J.M. Garcia, J.G. delaCampa, J. DeAbajo and T. A. Ezquerra. Relaxation behavior of aliphatic-aromatic poly(ether amide)s as revealed by dynamic mechanical and dielectric methods. *Journal of Polymer Science, Part B, Polymer Physics* Vol. 35(3) (1997), pp. 457-468.
- [8] Y.C. Yu, W.H. Jo and M.S. Lee. Segmented block copolyetheramides based on nylon 6 and polyoxypropylene. III. SAXS analysis. *Journal of Applied Polymer Science* Vol. 64(11) (1997), pp. 2155-2163.
- [9] B.B. Sauer, R.S. McLean, D.J. Brill and D.J. Londono. Morphology and orientation during the deformation of segmented elastomers studied with small-angle X-ray scattering and atomic force microscopy. *Journal of Polymer Science, Part B, Polymer Physics* Vol. 40(16) (2002), pp. 1727-1740.
- [10] B.B. Sauer, R.S. McLean and R.R. Thomas. Nanometer resolution of crystalline morphology using scanning probe microscopy. *Polymer International* Vol. 49(5) (2000), pp. 449-452.
- [11] S. Velankar and S.L. Cooper. Microphase Separation and Rheological Properties of Polyurethane Melts. 1. Effect of Block Length. *Macromolecules* Vol. 31(26) (1998), pp. 9181-9192.
- [12] B.B. Sauer, R.S. McLean, R.R. Thomas. *Polym Int* 2000, 49, 449-452.
- [13] M.J. Morin, E.V. Thompson. Proceedings of 3rd Int Conf on Pervaporation Process in Chemical Industry, Nancy, 1988, 349.

### Resume

Name: I-Kuan Yang, male. Research interests: rheology of liquid crystalline materials, rheology of nanosuspensions, rheological characterizations and structure changes of block copolymers.

